

Washington University School of Medicine

Digital Commons@Becker

2020-Current year OA Pubs

Open Access Publications

4-1-2023

Mitochondrial pyruvate carrier inhibition initiates metabolic crosstalk to stimulate branched chain amino acid catabolism

Daniel Ferguson

Sophie J Eichler

Nicole K H Yiew

Jerry R Colca

Kevin Cho

See next page for additional authors

Follow this and additional works at: https://digitalcommons.wustl.edu/oa_4

 Part of the [Medicine and Health Sciences Commons](#)

Please let us know how this document benefits you.

Authors

Daniel Ferguson, Sophie J Eichler, Nicole K H Yiew, Jerry R Colca, Kevin Cho, Gary J Patti, Trevor M Shew, Andrew J Lutkewitte, Sandip Mukherjee, Kyle S McCommis, Natalie M Niemi, and Brian N Finck

Mitochondrial pyruvate carrier inhibition initiates metabolic crosstalk to stimulate branched chain amino acid catabolism



Daniel Ferguson¹, Sophie J. Eichler¹, Nicole K.H. Yiew¹, Jerry R. Colca², Kevin Cho^{3,5}, Gary J. Patti^{1,3,4,5}, Trevor M. Shew¹, Andrew J. Lutkewitte¹, Sandip Mukherjee¹, Kyle S. McCommis⁶, Natalie M. Niemi⁷, Brian N. Finck^{1,*}

ABSTRACT

Objective: The mitochondrial pyruvate carrier (MPC) has emerged as a therapeutic target for treating insulin resistance, type 2 diabetes, and nonalcoholic steatohepatitis (NASH). We evaluated whether MPC inhibitors (MPCi) might correct impairments in branched chain amino acid (BCAA) catabolism, which are predictive of developing diabetes and NASH.

Methods: Circulating BCAA concentrations were measured in people with NASH and type 2 diabetes, who participated in a recent randomized, placebo-controlled Phase IIB clinical trial to test the efficacy and safety of the MPCi MSDC-0602K (EMMINENCE; NCT02784444). In this 52-week trial, patients were randomly assigned to placebo (n = 94) or 250 mg MSDC-0602K (n = 101). Human hepatoma cell lines and mouse primary hepatocytes were used to test the direct effects of various MPCi on BCAA catabolism in vitro. Lastly, we investigated how hepatocyte-specific deletion of MPC2 affects BCAA metabolism in the liver of obese mice and MSDC-0602K treatment of Zucker diabetic fatty (ZDF) rats.

Results: In patients with NASH, MSDC-0602K treatment, which led to marked improvements in insulin sensitivity and diabetes, had decreased plasma concentrations of BCAAs compared to baseline while placebo had no effect. The rate-limiting enzyme in BCAA catabolism is the mitochondrial branched chain ketoacid dehydrogenase (BCKDH), which is deactivated by phosphorylation. In multiple human hepatoma cell lines, MPCi markedly reduced BCKDH phosphorylation and stimulated branched chain keto acid catabolism; an effect that required the BCKDH phosphatase PPM1K. Mechanistically, the effects of MPCi were linked to activation of the energy sensing AMP-dependent protein kinase (AMPK) and mechanistic target of rapamycin (mTOR) kinase signaling cascades in vitro. BCKDH phosphorylation was reduced in liver of obese, hepatocyte-specific MPC2 knockout (LS-*Mpc2*^{-/-}) mice compared to wild-type controls concomitant with activation of mTOR signaling in vivo. Finally, while MSDC-0602K treatment improved glucose homeostasis and increased the concentrations of some BCAA metabolites in ZDF rats, it did not lower plasma BCAA concentrations.

Conclusions: These data demonstrate novel cross talk between mitochondrial pyruvate and BCAA metabolism and suggest that MPC inhibition leads to lower plasma BCAA concentrations and BCKDH phosphorylation by activating the mTOR axis. However, the effects of MPCi on glucose homeostasis may be separable from its effects on BCAA concentrations.

© 2023 The Author(s). Published by Elsevier GmbH. This is an open access article under the CC BY-NC-ND license (<http://creativecommons.org/licenses/by-nc-nd/4.0/>).

Keywords Pyruvate; Liver; Branched chain amino acids; Mitochondria; Diabetes

1. INTRODUCTION

The mitochondrial pyruvate carrier (MPC) has emerged as a therapeutic target for treating metabolic diseases including insulin resistance, type 2 diabetes, and nonalcoholic steatohepatitis (NASH) [1–5]. The MPC is a heterodimeric complex in the inner mitochondrial membrane that is composed of two proteins, MPC1 and MPC2 [6,7]. Given that pyruvate is synthesized primarily in the cytosol while the

enzymes that metabolize pyruvate (pyruvate carboxylase and pyruvate dehydrogenase (PDH)) are localized exclusively in the mitochondrial matrix, transport across the inner mitochondrial membrane is a critical step in the metabolism of this substrate. Pharmacologic inhibition or genetic deletion of the MPC in the liver has been shown to be beneficial in mouse models of insulin resistance, diabetes, and NASH [1–5]. Mitochondrial pyruvate metabolism is required for high rates of flux of pyruvate into the gluconeogenic pathway, which is markedly increased

¹Department of Medicine, Center for Human Nutrition, Washington University in St. Louis, United States ²Department of Biomedical Sciences, Western Michigan University School of Medicine, Kalamazoo, MI, Cirius Therapeutics, Kalamazoo, MI, United States ³Department of Chemistry, Washington University in St. Louis, United States ⁴Siteman Cancer Center, Washington University in St. Louis, United States ⁵Center for Metabolomics and Isotope Tracing, Washington University in St. Louis, United States ⁶Department of Biochemistry & Molecular Biology, Saint Louis University School of Medicine, United States ⁷Department of Biochemistry and Molecular Biophysics, Washington University in St. Louis, United States

*Corresponding author. MSC 8031-0014-01, 660 S. Euclid Avenue, St. Louis, MO 63110, United States. E-mail: bfinck@wustl.edu (B.N. Finck).

Received November 28, 2022 • Revision received February 12, 2023 • Accepted February 13, 2023 • Available online 18 February 2023

<https://doi.org/10.1016/j.molmet.2023.101694>

in diabetes [8], and MPCi improve glycemia by reducing hepatic glucose production [1,9]. However, there could be other molecular mechanisms mediating therapeutic effects that have yet to be identified.

In addition to the well-known effects on glucose homeostasis, insulin resistance and diabetes are also associated with perturbations in lipid and amino acid metabolism [8]. For example, plasma concentrations of valine, leucine, and isoleucine, which are classified as branched chain amino acids (BCAAs), are increased in people with obesity and insulin resistance [10–14], and high plasma BCAA concentrations are predictive of future development of diabetes [15]. Marked weight loss in people with obesity leads to reduced plasma BCAA concentrations [16,17]. Furthermore, dietary restriction of BCAAs in Zucker diabetic fatty (ZDF) rats lowers plasma BCAAs and improves insulin sensitivity [18], suggesting that high BCAA concentrations play a causative role in the development of insulin resistance. Consistent with this, genome-wide association studies in humans have demonstrated that genetic variations in genes encoding enzymes controlling BCAA metabolism are associated with increased BCAA concentrations and are also linked to the development of insulin resistance [19,20]. Strategies that correct accumulation of these bioactive amino acids may have value as therapeutic avenues for treating diabetes.

Circulating BCAA concentrations are regulated by dietary intake, rates of protein synthesis and proteolysis, and BCAA catabolism. To be oxidized, BCAAs are first converted to branched chain keto acids (BCKAs) by branched chain aminotransferases (BCAT). Next, BCKAs undergo oxidation that is catalyzed by the BCKA dehydrogenase (BCKDH) enzyme complex (E1, E2, and E3 subunits) localized in the mitochondrial matrix. BCKDH catalyzes a committed and rate-limiting step in BCAA catabolism [21]. BCKDH activity is regulated by inhibitory phosphorylation of serine 293 of the E1 alpha subunit (pBCKDH), which is mediated by a BCKDH kinase (BDK). Conversely, BCKDH is activated by a protein phosphatase (PPM1K) that removes this covalent modification [21]. Mechanistic studies conducted over the past several years have demonstrated that the phosphorylation of BCKDH is increased in the liver of rodent models of obesity/diabetes (*ob/ob* and ZDF rats) [22,23], suggesting that impairments in BCKA catabolism may drive the accumulation of BCAAs in obesity. The increase in pBCKDH content seems to be mediated by reduced PPM1K and increased BDK activity [23] and genetic or pharmacologic approaches to suppress BDK activity or overexpress PPM1K are effective at enhancing BCKA catabolism and improving glucose intolerance in rodent models of obesity [24].

In this work we examined the potential effects of MPC inhibition on BCAA metabolism by using pharmacologic and genetic approaches and explored the molecular mechanisms involved. These studies unveiled interesting metabolic crosstalk between the mitochondrial metabolism of pyruvate and BCKAs. Moreover, these studies suggest that part of the metabolic benefit derived from MPC inhibition could be mediated by stimulating the catabolism of BCAAs.

2. METHODS

2.1. Study design

EMMINENCE [ClinicalTrials.gov Identifier: NCT02784444] was a randomized, double-blind evaluation of safety and potential efficacy of MSDC-0602K in patients with type 2 diabetes and liver injury, assessing 3 oral daily doses of MSDC-0602K or placebo given for 12 months to adult patients with biopsy-proven NASH, with fibrosis and without cirrhosis [3]. The patients were stratified for the co-diagnosis of type 2 diabetes and severity of fibrosis. Approximately 50% of the

patients were diabetic and approximately 60% had advanced fibrosis of F2 or F3. The primary efficacy endpoint was assessed at 12 months. In the EMMINENCE study, the effects of MSDC-0602K on liver histology and liver and glucose metabolism markers were tested in patients with NASH diagnosed by liver biopsy, with and without T2D. The plasma concentrations of selected amino acid in patients receiving placebo or high dose (250 mg/day) MSDC-0602K were determined using NMR-based amino acid quantification as described previously [25]. The study was conducted in accordance with ICH GCP and all applicable regulatory requirements. Patients provided written informed consent prior to study participation. The protocol and consent forms were approved by relevant institutional review boards.

2.2. Animal studies

All animal experiments were approved by the Institutional Animal Care and Use Committee of Washington University in St. Louis (animal protocol number 20–0004). Male and female hepatocyte-specific MPC2 knockout (*LS-Mpc2*^{−/−}) and leptin receptor deficient (*db/db* *LS-Mpc2*^{−/−}) mice were generated as previously described [1]. Littermates that did not express Cre were used as controls in all studies. For high fat diet studies, male mice were switched from standard chow to a 60% high fat diet (Research Diets Inc, #D12492) at 6 weeks of age and were maintained on diet for 20 weeks. Prior to sacrifice for tissue and blood collection, animals were fasted for 5 h. Glucose tolerance testing was performed after a 5 h fast, then mice were injected i. p. with D-glucose (1 g/kg body weight), after an initial blood glucose measurement (time = 0). Glucose was monitored at indicated time points with a handheld glucose meter (Contour Next, Bayer). Obese (*fa/fa*) and lean (*fa/+*) Zucker diabetic fatty (ZDF) rats were purchased from Charles River (Strain Code 370 [Obese *fa/fa*] and 371 [Lean *fa/+*]). At approximately 8 weeks of age, rats were given ad libitum access to a diet composed of repelleted Purina 5008 (Research Diets C13000) or Purina 5008 with or without MSDC-0602K at 330 parts per million (Research Diets C21092001). After 3 weeks on these diets, rats were fasted for 5 h, then sacrificed for tissue and blood collection.

2.3. Cell culture experiments

Huh7 and HepG2 human hepatoma cells were maintained in DMEM (ThermoFisher Cat# 11965092) supplemented with 10% fetal bovine serum, pyruvate (1 mM), and Penicillin-Streptomycin (100 U/mL). For inhibitor studies, cells were treated overnight in serum-free culture media containing indicated treatments. The following day, cells were starved in DMEM containing no serum, glucose, or amino acids (MyBioSource Cat# MBS6120661) with indicated treatments for 2 h, and then harvested for protein.

Primary hepatocytes were isolated from wild-type *Mpc2*^{fl/fl} mice as previously described [9]. Following cannulation of the portal vein and collagenase digestion, cells were counted and plated in 6-well collagen-coated plates in DMEM supplemented with 10% fetal bovine serum, pyruvate (1 mM), and Penicillin-Streptomycin (100 U/mL). After 3–4 h, cells were treated overnight in culture media containing indicated treatments. The following day, cells were starved in DMEM containing no serum, glucose, or amino acids (MyBioSource Cat# MBS6120661) with indicated treatments for 2 h, and then harvested for protein.

All drugs were solubilized in DMSO and added at an equal volume to vehicle (DMSO), which was no more than 0.1% of volume in media. Reagents were obtained from the following companies: UK5099 (Cayman); 7ACC2 (Cayman); Zaprinast (Sigma); MSDC-0602K (Cirius Therapeutics); BT2 (Sigma); dichloroacetate (Sigma); Ketoisovaleric

acid (KIV) [$1-^{14}\text{C}$] sodium salt (American Radiolabeled Chemicals, ARC 3191), Dorsomorphin (Cayman), Torin1 (Cayman), Rapamycin (Cayman), MK2206 (Selleckchem), SGK1 inhibitor (Cayman), and Rottlerin (Selleckchem). For siRNA experiments, Huh7 cells were transfected with Silencer™ Pre-Designed siRNAs (ThermoFisher): Silencer™ Negative Control No. 1 siRNA (Cat# AM4611); Ppm1k^{#1} (Cat# AM16708; siRNA ID:127997); Ppm1k^{#2} (Cat# AM16708; siRNA ID:127999); BDK^{#1} (Cat# AM16708; siRNA ID:110905); BDK^{#2} (Cat# AM16708; siRNA ID:140032); mTOR (Cat# AM51331; siRNA ID: 603); Raptor (Santa Cruz# 44069); or Rictor (Santa Cruz# 61478) using Lipofectamine RNAiMAX Transfection Reagent (ThermoFisher) according to manufacturer's instructions. After 48 h, cells were treated as previously mentioned for inhibitor experiments. After 48 h, media was replaced with serum-free DMEM with indicated treatments as previously mentioned above.

2.4. BCKA oxidation assay

We performed BCKA oxidation assays by using [^{14}C]-KIV as previously described [26], with minor modifications. Huh7 cells were plated in 3.5 cm dishes at ~70–80% confluency. The following day, media was replaced with serum-free culture media with indicated treatments overnight. The following day, media was replaced with amino acid free media with DMSO (vehicle), 7ACC2 (2.5 μM), or MSDC-0602K (25 μM), and incubated for 1 h [^{14}C]-KIV was added (0.065 μCi), then the dish was quickly placed into an airtight CO_2 collection chamber (Fisher Nalgene® style 2118 jar, fitted with a rubber stopper (Kontes 774,250–0014), and a center-well hanging bucket (Kimble 882,320–0000) containing Whatman filter paper soaked with 50 μL benzothonium hydroxide (Sigma)). After 30 min at 37 °C, the reaction was terminated by 100 μL of 0.5 M H_2SO_4 , injected using a syringe. [^{14}C]- CO_2 liberation was allowed to proceed for an additional 30 min on ice, then the center-well collection bucket was cut and put into a liquid scintillation vial. Production of [^{14}C]- CO_2 was determined via a scintillation counter and normalized to cellular protein, determined using DC protein assay (Bio-Rad).

2.5. Mouse and rat plasma amino acid quantification

Amino acids were extracted from 20 μL of plasma with 200 μL of methanol containing leucine-d3 (320 ng), isoleucine- $^{13}\text{C}_6$, ^{15}N (160 ng), and valine-d8 (400 ng) as internal standards for Leu, Ile, and Val, respectively. Quality control (QC) samples were prepared by pooling aliquots of study samples and injected every four study samples to monitor instrument performances throughout these analyses. The analysis of amino acids was performed on a Shimadzu 20AD HPLC system and a SIL-20AC autosampler coupled to 4000Qtrap mass spectrometer (AB Sciex) operated in positive multiple reaction monitoring (MRM) mode. Data processing was conducted with Analyst 1.6.3 (Applied Biosystems). The relative quantification data for all analytes were presented as the peak ratio of each analyte to the internal standard.

For plasma levels of 3-hydroxybutyrate and acylcarnitines, 180 μL of methanol:acetonitrile:water (2:2:1) was added to 20 μL of plasma, vortexed for 1 min, stored at $-20\text{ }^\circ\text{C}$ for 1 h, then centrifuged at $14,000\times g$ and $4\text{ }^\circ\text{C}$, then the supernatant was transferred to LC vials and stored at $-80\text{ }^\circ\text{C}$ until MS analysis. 3-hydroxybutyrate was measured by ultra-high-performance LC (UHPLC)/MS, as described below for LC/MS analysis of cell metabolites.

Plasma levels of acylcarnitines were measured as described previously [27]. Acylcarnitines were separated on an Acquity UPLC HSS T3 column ($2.1 \times 150\text{ mm}$, $1.8\text{ }\mu\text{m}$) including an Acquity UPLC HSS T3 VanGuard Pre-Column ($2.1 \times 5\text{ mm}$, $1.8\text{ }\mu\text{m}$) at a temperature of

$60\text{ }^\circ\text{C}$ and a flow rate of $250\text{ }\mu\text{L}\cdot\text{min}^{-1}$. The mobile phases consisted of A: 60% acetonitrile, 40% water, 0.1% formic acid, 10 mM ammonium formate, 2.5 μM medronic acid, and B: 90% 2-propanol, 10% acetonitrile, 0.1% formic acid, 10 mM ammonium formate. The following linear gradient was used: 0–2 min, 30% B; 17 min, 75% B; 20 min, 85% B; 23–26 min, 100% B; 26 min, 30% B followed by a re-equilibration phase of 5 min. Acylcarnitines were detected in positive ion mode.

2.6. Metabolomics extraction and LC/MS analysis of cell metabolites

Huh7 cells were treated overnight in serum-free culture media containing indicated treatments. The following day, cells were starved in DMEM containing no serum, glucose, or amino acids with indicated treatments for 2 h described in the text then metabolites were extracted as previously described [28]. Briefly, media was removed and collected (described below) and cells were washed three times with PBS and three times with HPLC-grade water. Subsequently, cells were quenched with ice cold HPLC-grade methanol, then scraped and transferred to Eppendorf tubes. Samples were dried in a SpeedVac for 2–6 h. Dried samples were reconstituted in 1 mL of ice cold methanol:acetonitrile:water (2:2:1), and subjected to three cycles of vortexing, freezing in liquid nitrogen, and 10 min of sonication at $25\text{ }^\circ\text{C}$. Next, samples were then stored at $-20\text{ }^\circ\text{C}$ for at least 1 h then centrifuged at $14,000\times g$ and $4\text{ }^\circ\text{C}$. Supernatants were transferred to new tubes and dried by SpeedVac for 2–5 h. To normalize across samples, protein content of cell pellets was measured using the BCA kit (ThermoFisher). After drying the supernatant, 1 mL of water:acetonitrile (1:2) was added per 2.5 mg of cell protein, determined in pellets obtained after extraction. Samples were subjected to two cycles of vortexing and 10 min of sonication at $25\text{ }^\circ\text{C}$. Next, samples were centrifuged at $14,000\times g$ and $4\text{ }^\circ\text{C}$ for 10 min, transferred supernatant to LC vials, and stored at $-80\text{ }^\circ\text{C}$ until MS analysis.

Media was collected and transferred to Eppendorf tubes. Following a brief centrifugation at $4\text{ }^\circ\text{C}$ to remove dead cells, 900 μL of methanol:acetonitrile:water (2:2:1) was added to 100 μL of media then vortexed for 1 min, stored at $-20\text{ }^\circ\text{C}$ for 1 h, then centrifuged at $14,000\times g$ and $4\text{ }^\circ\text{C}$, then the supernatant was transferred to LC vials and stored at $-80\text{ }^\circ\text{C}$ until MS analysis.

Ultra-high-performance LC (UHPLC)/MS was performed with a ThermoScientific Vanquish Horizon UHPLC system interfaced with a ThermoScientific Orbitrap ID-X Tribrid Mass Spectrometer (Waltham, MA). Hydrophilic interaction liquid chromatography (HILIC) separation was accomplished by using a HILICON iHILIC-(P) Classic column (Tvistevagen, Umea, Sweden) with the following specifications: $100 \times 2.1\text{ mm}$, $5\text{ }\mu\text{m}$. Mobile-phase solvents were composed of A = 20 mM ammonium bicarbonate, 0.1% ammonium hydroxide and 2.5 μM medronic acid in water:acetonitrile (95:5) and B = 2.5 μM medronic acid in acetonitrile:water (95:5). The column compartment was maintained at $45\text{ }^\circ\text{C}$ for all experiments. The following linear gradient was applied at a flow rate of $250\text{ }\mu\text{L}\cdot\text{min}^{-1}$: 0–1 min: 90% B, 1–12 min: 90–35% B, 12–12.5 min: 35–25% B, 12.5–14.5 min: 25% B. The column was re-equilibrated with 20 column volumes of 90% B. The injection volume was 2 μL for all experiments.

Data were collected with the following settings: spray voltage, -3.0 kV ; sheath gas, 35; auxiliary gas, 10; sweep gas, 1; ion transfer tube temperature, $250\text{ }^\circ\text{C}$; vaporizer temperature, $300\text{ }^\circ\text{C}$; mass range, 67–1500 Da, resolution, 120,000 (MS1), 30,000 (MS/MS); maximum injection time, 100 ms; isolation window, 1.6 Da. LC/MS data were processed and analyzed with the open-source Skyline software [29].

2.7. Immunoblotting

Western blotting was performed as previously described [28] using RIPA lysis buffer (Cell Signaling Technology) with added protease and phosphatase inhibitors (Cell Signaling Technology). For tissue, ~30 mg of tissue was homogenized using a TissueLyser. For in vitro experiments, cells were scraped in lysis buffer then briefly sonicated. Lysates were normalized to protein concentration, denatured, and run on NuPAGE precast 4–12% Bis-Tris gels with MOPS buffer then transferred to Immobilon PVDF. Antibodies used were: Phospho-BCKDH-E1 α Ser293 (Cell Signaling Technology (CST) 40,368), BCKDH-E1 α (CST 90198), Phospho-ACLY Ser455 (CST 4331), ACLY (CST 4332), Phospho-AMPK α Thr172 (CST 2535), AMPK α (CST 2603), Phospho-Akt Ser473 (CST 4060), Akt (CST 2920), Phospho-mTOR Ser2448 (CST 2971), mTOR (CST 4517), Phospho-S6 Ribosomal Protein Ser235/236 (CST 4858), S6 Ribosomal Protein (CST 2317), MPC1 (CST 14462), MPC2 (CST 46141), Raptor (CST 2280), Rictor (CST 2114), COXIV (CST 11967), H3 (CST 14269), HSP60 (CST 12165), β -Actin (CST 3700), Phospho-ACC Ser79 (EMD Millipore 07–303), ACC (EMD Millipore 05–1098), Phospho-PDH α 1 Ser293 (EMD Millipore AP1062), and PDH (CST 3205); BDK (sc-374,425) and PPM1K (sc-514,925); and α -Tubulin (Sigma T8203). Images were obtained using the Licor system with Image Studio Lite software.

2.8. mTOR phospho antibody array

Huh7 cells were treated overnight in serum-free culture media containing indicated treatments. The following day, cells were starved in DMEM containing no serum, glucose, or amino acids with indicated treatments for 2 h then samples used for the mTOR Phospho Antibody Array (Full Moon Biosystems PMT138) according to manufacturer's instructions.

2.9. Plasma and liver triglyceride quantification

Plasma triglyceride levels were measured using a commercially available kit (Thermo Scientific™).

Liver triglyceride levels were measured by homogenizing ~100 mg frozen liver tissue in ice cold PBS, then solubilizing lipids in 1% sodium deoxycholate and measured using a commercially available kit (Thermo Scientific™) as previously described [30].

2.10. Statistical analyses

Figures were generated using GraphPad Prism Software version 9.0.1 for windows. All data and are presented as the mean \pm SEM. Statistical significance was calculated using an unpaired Student's t-test, two-way analysis of variance (ANOVA) with repeated measures, or one-way ANOVA with Tukey's multiple comparisons test, with a statistically significant difference defined as $p < 0.05$.

3. RESULTS

3.1. MPCi treatment reduced plasma BCAA concentrations in people with NASH

Recently, a randomized, placebo-controlled, Phase IIB clinical trial of an MPCi (MSDC-0602K) in people with NASH (EMMINENCE; NCT02784444) was conducted [3]. We examined a variety of plasma parameters in patients treated with placebo ($n = 94$) or 250 mg ($n = 101$) MSDC-0602K per day for one year. As previously reported [3], one year of treatment with MSDC-0602K led to lower insulin and glucose concentrations and increased adiponectin concentrations when compared to baseline values, whereas placebo treatment had no effect (Table 1). Since levels of BCAAs are elevated in people with obesity and insulin resistance [10–14], we next examined BCAA

Table 1 — Subject characteristics and plasma chemistry.

	placebo	250 mg
Age	54.6 \pm 11.2	56.8 \pm 10.4
Sex (M/F)	43/51	43/58
N	94	101
Glucose (mM)		
Mean difference	0.6211 \pm 2.344	−0.6759 \pm 2.449*
N	76	87
Insulin (μ U/ml)		
Mean difference	2.28 \pm 26.99	−7.601 \pm 15.03*
N	75	82
Adiponectin (ng/ml)		
Mean difference	1796 \pm 2017	6587 \pm 5514*
N	75	83

Data are means from baseline \pm SEM; * $p < 0.05$ versus placebo.

concentrations by using NMR and found that MSDC-0602K led to lower concentrations of valine, leucine, isoleucine and total BCAA, while placebo had no effect (Figure 1). Finally, people treated with MSDC-0602K exhibited decreased concentrations of plasma alanine, while plasma glycine, which has been shown to be lower in T2DM, tended to increase ($p = 0.0863$) (Figure 1). Collectively, these data suggest that the MPCi MSDC-0602K reduces plasma BCAA concentrations in people with NASH.

3.2. Inhibition of the MPC increases BCKA oxidation and reduces BCKDH phosphorylation in vitro

Oxidation of BCKA in the BCKDH complex is an irreversible and rate-limiting step in BCAA catabolism and impairments in this process may play a causative role in elevated BCAA concentrations observed in obesity. We sought to determine if MPCi could directly affect BCAA/BCKA oxidation in an in vitro system by quantifying conversion of radiolabeled 14 C-ketoisovaleric acid (ketovaline) into 14 CO $_2$ in human hepatoma cells (Huh7 cells). Treatment of Huh7 cells with 7ACC2, a potent MPCi that is structurally unrelated to MSDC-0602K, or MSDC-0602K lead to a significant 32% and 43% increase in BCKDH oxidation relative to vehicle, respectively (Figure 2A). In addition, we quantified intermediary metabolites from Huh7 cells treated with MPCi (UK5099 or 7ACC2). We detected an increase in ketovaline levels, and found trends toward increases in downstream BCAA catabolites including hydroxyisobutyrate, propionyl CoA, and methylmalonyl CoA (Figure 2B). We also observed substantial decreases in levels of various TCA intermediates including citrate, fumarate, and malate, which is consistent with a suppression of pyruvate entry into the TCA cycle (Figure 2B). Interestingly, we found that extracellular pyruvate was increased in the media of cells treated with 7ACC2 (Supplementary Fig. 1). TCA intermediates were among the most reduced metabolites that were examined, whereas levels of methionine and nucleotide monophosphates (GMP, UMP, and CMP) were highly elevated in response to MPCi treatment (Figure 2C). Importantly, as depicted in the heatmap, both MPCi (UK5099 and 7ACC2) produced similar changes in metabolite abundance, confirming the reproducibility of our results (Figure 2B–C). Overall, these data suggest that MPCi lead to increased BCKDH activity and BCAA catabolism in vitro.

The rate-limiting enzyme in BCAA catabolism is the mitochondrial branched chain ketoacid dehydrogenase (BCKDH) that is deactivated by phosphorylation (Figure 3A). Using human hepatoma cell lines (Huh7 and HepG2), we tested the effects of several MPCi including UK5099, 7ACC2, zaprinast, and MSDC-0602K on BCKDH phosphorylation. Overnight treatment of serum-starved hepatoma cells with the various MPCi resulted in substantial decreases in pBCKDH, relative to

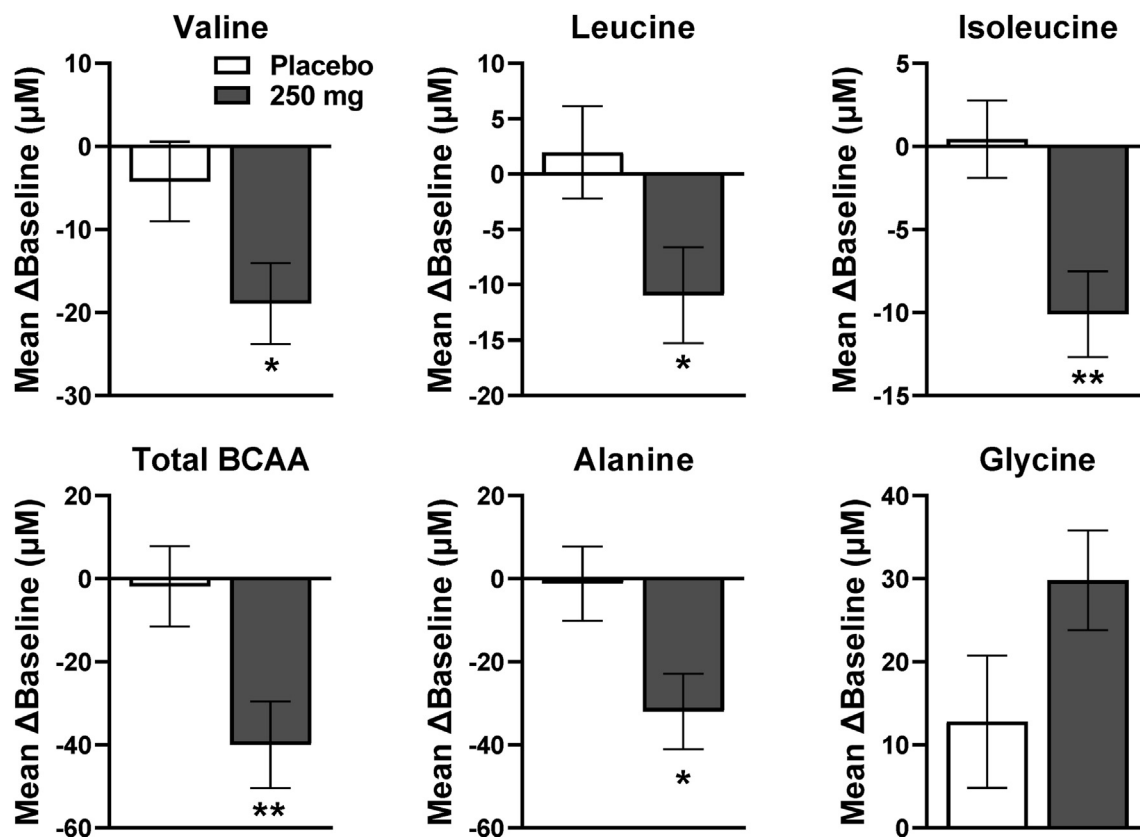


Figure 1: MPCi treatment reduced plasma BCAA concentrations in people with NASH. Change in the concentrations of amino acids from baseline, after 12 months with placebo or MSDC-0602K (250 mg/day) (Mean and SEM; ANOVA for dose versus placebo * $p < 0.05$, ** $p < 0.01$).

vehicle-treated Huh7 cells (Figure 3B). 7ACC2 also reduced BCKDH phosphorylation in HepG2 cells (Supplemental Fig. 2A). Since hepatoma cells have metabolic features not observed in hepatocytes in vivo, we isolated primary mouse hepatocytes from wild-type mice and treated them with the MPCi UK5099. Like human hepatoma cell lines, we found that BCKDH phosphorylation was decreased in MPCi-treated primary hepatocytes (Figure 3C). BCKDH phosphorylation is controlled by a BCKDH kinase (BDK) and a corresponding phosphatase PPM1K (aka PP2Cm or PP2Ckappa) [21] (Figure 3A). Recent work has suggested that BDK and PPM1K also directly phosphorylate and dephosphorylate, respectively, ATP citrate lyase (ACLY), a key enzyme involved in de novo lipogenesis at serine 455 [24]. Interestingly, the phosphorylation of ACLY at serine 455 (pACLY) was increased by each of the MPCi tested and in mouse primary hepatocytes (Figure 3B–C), suggesting that the effect of MPCi is specific to the phosphorylation of BCKDH.

Additionally, the effect of MPCi was dose-dependent, with marked decreases in BCKDH phosphorylation being observed in the nanomolar (UK5099 and 7ACC2) and micromolar (MSDC-0602K) range (Figure 3D and Supplemental Fig. 2B). These dose effects are consistent with the established relative potency of these compounds as MPCi [2,9]. Further, since the average trough levels of MSDC-0602K and its active metabolite at the 250 mg dose were approximately 6.2 μM [3], these effects could be relevant in vivo. Lastly, we performed a time-course study and saw observable decreases in pBCKDH with as little as 30 min of MPCi treatment (Figure 3E). Compared to the effect of MPCi to decrease pBCKDH, the increase in pACLY caused by MPCi was similarly dose- and time-dependent.

3.3. PPM1K mediates the effects of MPCi on BCKDH phosphorylation

To determine whether MPCi might be regulating BCKDH phosphorylation through BDK, we tested whether BT2, a chemical inhibitor of BDK, would impact the effects of MPCi. As can be seen in Figure 3F, treatment with either a low or high dose of BT2 reduced pBCKDH in vehicle-treated cells. However, MPCi treatment had an additive and quantitatively greater effect even with high dose BT2 (Figure 3F), suggesting that the effect of MPCi is not mediated by inhibition of BDK. To confirm this, we used siRNA to selectively diminish expression of either PPM1K or BDK. Western blotting confirmed decreased protein expression of PPM1K or BDK with the respective siRNA (Figure 3G). MPCi-treatment yielded a comparable reduction in pBCKDH levels in both control and BDK siRNA treated cells; again, suggesting a BDK-independent effect. In contrast, PPM1K siRNA markedly blunted the effects of 7ACC2 on BCKDH phosphorylation (Figure 3G), suggesting that MPCi-induced effects on pBCKDH are mediated via the PPM1K phosphatase. Notably, the MPCi-mediated increase in pACLY was not diminished with either BDK or PPM1K knockdown or by BT2 treatment (Figure 3F–G).

3.4. MPCi activate the energy-sensing kinases AMPK and mTOR to mediate the effect on BCKDH

Previous studies have shown that pyruvate and glucose negatively regulate BCKDH activity in the perfused rat heart [31,32]. This effect was reversed by treatment with early MPCi or dichloroacetate (DCA), which inhibits pyruvate dehydrogenase kinase to stimulate pyruvate oxidation by dephosphorylation of the PDH enzyme. We hypothesized

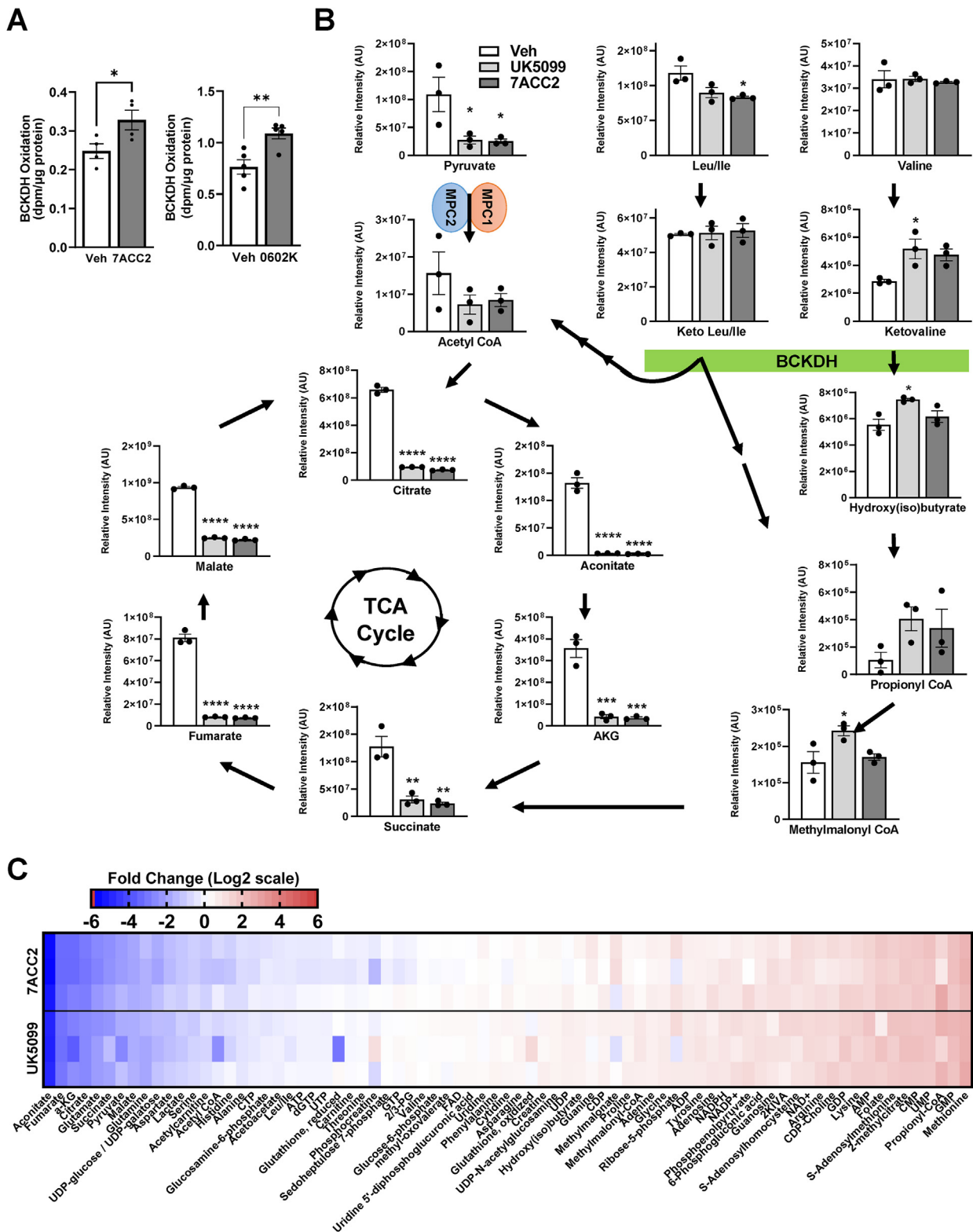


Figure 2: BCKDH oxidation and BCAA catabolism are increased with MPC inhibition. (A) BCKA oxidation assay performed in Huh7 cells treated with either Veh, 7ACC2 (2.5 μ M), or MSDC-0602K (25 μ M). (B) Analysis of metabolites performed after cells were treated with either Veh (DMSO), UK-5099 (2.5 μ M), or 7ACC2 (2.5 μ M). All data were corrected to protein content and are expressed as mean \pm SEM. * p < 0.05, ** p < 0.01, *** p < 0.001, **** p < 0.0001. (C) Heatmap of metabolites expressed as fold change (Log₂ scale) relative to Veh group.

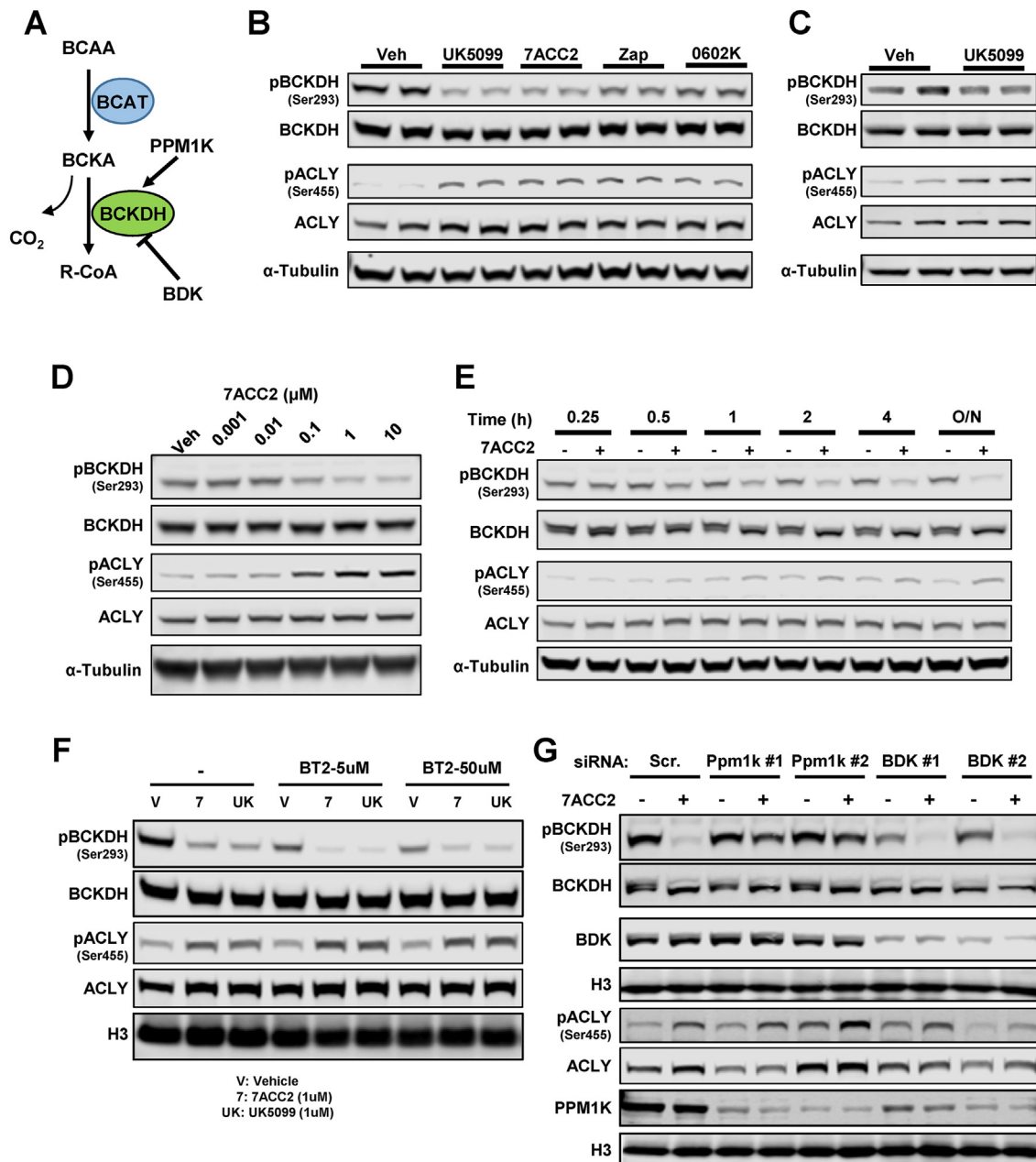


Figure 3: Inhibition of the MPC reduces BCKDH phosphorylation in vitro. (A) Schematic showing the oxidative decarboxylation of BCKA, releasing CO₂, by BCKDH that is regulated via an inhibitory phosphorylation by BDK, or an activating dephosphorylation by PPM1K. Representative western blots of pBCKDH-S293, BCKDH, pACLY-S455, ACLY, and α-Tubulin. (B) Huh7 cells were treated with MPCi Veh (DMSO), UK-5099 (1 μM), 7ACC2 (1 μM), Zaprinast (Zap, 10 μM), and MSDC-0602K (10 μM). (C) Primary hepatocytes were isolated from wild-type mice and treated with either Veh (DMSO) or UK5099 (2.5 μM). (D) Cells were treated overnight with indicated concentration of MPCi. (E) Veh or 7ACC2 (2.5 μM) was added at the indicated time points before harvested for western blotting. (F) Cells were treated with Veh or MPCi, in the absence or presence of the BDK inhibitor BT2 overnight, at indicated concentrations. (G) Cells were transfected with indicated siRNA, then 48 h later were treated with either Veh or 7ACC2 overnight.

that MPCi could be preventing the accumulation of high intramitochondrial levels of pyruvate, thus avoiding the inhibitory effects of pyruvate on BCKDH activity. Addition of pyruvate to the media of Huh7 cells resulted in increased BCKDH and PDH phosphorylation (Figure 4A). As expected, DCA reduced PDH phosphorylation and, interestingly, 7ACC2 treatment also reversed the effect of pyruvate on PDH phosphorylation. Treatment with 7ACC2 or DCA mostly blocked the effects of added pyruvate on pBCKDH and led to a substantial decrease in pBCKDH with both vehicle and MPCi treatment (Figure 4A). Taken together, these data indicate that MPCi likely decreases

intramitochondrial pyruvate levels, consequently preventing the inhibitory effects of pyruvate on BCKDH activity.

Alternatively, or in addition, the effects of MPCi on pBCKDH could be mediated by compensatory changes in mitochondrial energy homeostasis. As its name suggests, the energy-sensing AMP-activated protein kinase (AMPK) is activated by elevated AMP concentrations [33]. Metabolomic analyses of Huh7 cells treated with either UK-5099 or 7ACC2 revealed increased AMP and an increased AMP/ATP ratio, compared to vehicle controls (Figure 4B). Consistent with this, MPCi treatment led to a slight increase in the phosphorylation of the α

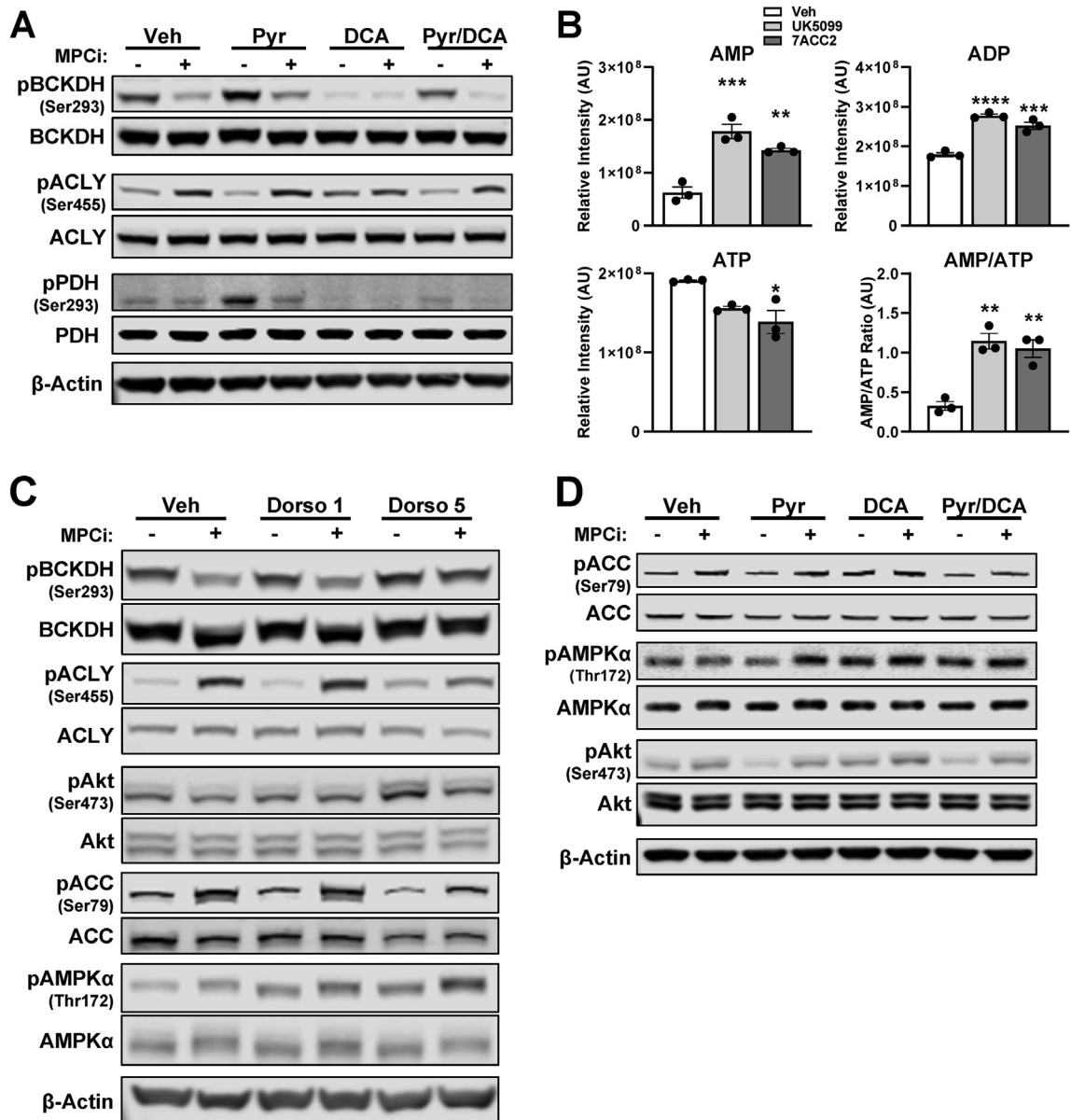


Figure 4: MPCi activate the energy-sensing kinases AMPK to mediate the effect on BCKDH. (A) Cells were treated with Veh or 7ACC2 (2.5 μ M), in the absence or presence of pyruvate (1 mM) and/or dichloroacetate (DCA, 20 mM) overnight. (B) Analysis of metabolite levels performed on cells treated with either Veh (DMSO), UK5099 (2.5 μ M), or 7ACC2 (2.5 μ M). All data are expressed as mean \pm SEM. * $p < 0.05$, ** $p < 0.01$, *** $p < 0.001$, **** $p < 0.0001$. (C) Cells were treated with Veh or MPCi, in the absence or presence of the AMPK inhibitor dorsomorphin at concentrations of either 1 μ M (Dorso 1) or 5 μ M (Dorso 5). (D) Representative blots of cells were treated with Veh or 7ACC2 (2.5 μ M), in the absence or presence of pyruvate (1 mM) and/or dichloroacetate (DCA, 20 mM) overnight.

subunit of AMPK and a more prominent increase in the phosphorylation of the AMPK target acetyl-CoA carboxylase (pACC) at serine 79 (Figure 4C). Treatment with the AMPK inhibitor, dorsomorphin, at concentrations that blocked most of the effect of MPCi on pACC also inhibited the effect of MPCi on pBCKDH and attenuated the effect on pACLY (Figure 4C). Interestingly, the inhibition of PDKs with DCA also increased pACC, but this was somewhat attenuated when pyruvate was added with DCA (Figure 4D). These data suggest that inhibition of the MPC leads to an activation of AMPK that mediates the metabolic crosstalk leading to reduced pBCKDH.

The lack of glutamine in the amino acid-free media supplied to cells during MPCi treatment 1–2 h prior to harvest could produce TCA insufficiency. We therefore looked at the effects of titrating in various

amounts of glutamine during this time. Adding back higher concentrations of glutamine (≥ 0.2 mM) blunted the effect of MPC inhibition on pBCKDH and pACLY, as well as pACC at the highest concentration (2 mM) in Huh7 cells, suggesting that stimulating glutaminolysis may overcome the effect of MPC inhibition (Supplementary Fig. 3).

3.5. MPCi treatment activates mTORC2 signaling, which is required for reduced pBCKDH

The mechanistic target of rapamycin (mTOR) kinase is another nutrient sensing signaling cascade that can mediate effects through two multi-subunit complexes (mTORC1 and mTORC2) that control a variety of cellular and metabolic processes [34]. Prior work has demonstrated that AMPK is a direct activator of mTORC2 [35]. We hypothesized that

mTORC2 might be activated by MPCi because ACLY phosphorylation at serine 455 is known to be enhanced by mTORC2 activation [36,37], which could explain why pACLY was increased with MPCi treatment (Figure 3B). Indeed, we found that phosphorylation of AKT at serine 473 (pAKT), which is a known target of mTORC2, was decreased by pyruvate treatment and increased in cells treated with MPCi or DCA (Figure 4D).

We next examined the effects of treating cells with UK-5099 on mTORC pathway activation using an mTOR phospho antibody array. As predicted, the array indicated that the phosphorylation of AMPK was increased (Figure 5A), confirming our previous results (Figure 4C), and revealed increased phosphorylation of several mTOR targets (Figure 5A). Furthermore, treatment with rapamycin, which is partially selective for mTORC1, somewhat attenuated the effect of MPCi on pBCKDH and pACLY (Figure 5B). However, Torin1, which inhibits both mTORC1 and mTORC2, completely blocked the effect of MPCi on pBCKDH and markedly attenuated the increased phosphorylation of pACLY in Huh7 cells (Figure 5B). We attempted to block the effect of MPCi by siRNA-mediated suppression of mTOR signaling by knocking down key components of mTORC1 (Raptor) or mTORC2 (Rictor) complexes. Interestingly, knocking down either Raptor or Rictor had no effect on the ability of MPCi to reduce pBCKDH and increase pACLY (Figure 5C). However, siRNA directed against the mTOR kinase itself, blocked the effect of MPCi on these serine phosphorylation events like the effect of Torin1 (Figure 5C). These data could suggest that either mTORC1 or mTORC2 is sufficient to mediate the metabolic crosstalk or, alternatively, that additional mTOR complexes may exist, which has been suggested [38].

To further investigate how mTOR may mediate the metabolic crosstalk of MPCi, we tested the role of several downstream effectors of mTORC2, which have been demonstrated to localize to the mitochondria (AKT [39], serum/glucocorticoid regulated kinase (SGK) [40], and protein kinase C (PKC)). As seen in Figure 5D, inhibitors to AKT and SGK did not alter the effect of MPCi on BCKDH phosphorylation. In contrast, the PKC inhibitor rottlerin appreciably blunted the decrease in MPCi-mediated pBCKDH (Figure 5D), suggesting that PKC could be an important downstream regulator of MPC inhibition.

Interestingly, treatment of cells with Torin1 also blunted the effects of MPCi on pACC (Figure 5E) whereas inhibition of AMPK did not attenuate the effects of MPCi on pAKT content (Figure 4C). These data potentially indicate that AMPK activation lies downstream of mTOR activation or is activated indirectly due to metabolic effects of mTOR signaling in the setting of MPC inhibition.

3.6. Genetic deletion of the MPC in liver of mice reduces BCKDH phosphorylation

To investigate the effect of MPC deletion on BCKDH phosphorylation in vivo, we performed western blotting for hepatic pBCKDH in wild-type and hepatocyte-specific MPC2 knockout (*LS-Mpc2*^{-/-}) mice fed a 60% high fat diet for 20 weeks. Not only did *LS-Mpc2*^{-/-} mice have an improvement in glucose tolerance (Figure 6A), these mice had a 45% decrease in levels of hepatic pBCKDH compared to wild-type mice (Figure 6B–C). Importantly, *LS-Mpc2*^{-/-} mice also exhibited increased pACLY and pAKT, consistent with our in vitro observations (Figure 6B–C). However, we found no difference in the abundance of plasma BCAAs between groups, but did observe an increase in keto-valine (Supplementary Figs. 4A–B). Unlike our in vitro studies, there were no differences in hepatic pACC or pAMPK in these mice (Figure 6B and Supplementary Fig. 4C).

We further tested this in a genetic model of obesity by crossing *LS-Mpc2*^{-/-} mice on to the *db/db* background. Liver MPC deletion in *db/*

db mice has previously been shown to lower blood glucose concentrations and improve glucose tolerance [1]. The *db/db* mice had a substantial increase in liver pBCKDH levels and loss of *Mpc2*^{-/-} in hepatocytes slightly, but significantly, decreased BCKDH phosphorylation (Supplementary Fig. 5A). We also observed increased pACLY in the liver of *LS-Mpc2*^{-/-} on the *db/db* background, compared to wild-type *db/db* mice, but detected no change in pAKT or pACC (Supplementary Fig. 5A). Plasma leucine, valine, and total BCAA levels were elevated in *db/db* mice, compared to lean controls, whereas only valine levels were elevated in *LS-Mpc2*^{-/-} on the *db/db* background (Supplemental Fig. 5B). Collectively, these data demonstrate that hepatocyte-specific deletion of MPC2 leads to decreased BCKDH phosphorylation (indicative of increased activity) in both dietary and genetic models of obesity/hyperglycemia.

3.7. Pharmacological MPC inhibition in diabetic rats improves hyperglycemia

Next, we investigated the effect of the pharmacological MPC inhibitor MSDC-0602K in Zucker diabetic fatty (ZDF; *fa/fa* genotype) rats. MSDC-0602K was incorporated into rodent chow (330 ppm) and fed to *fa/fa* rats for a period of 3 weeks. After 3 weeks of feeding, *fa/fa* rats fed chow containing vehicle or MSDC-0602K were significantly heavier than lean (*fa/+*) control rats, by 23% and 59%, respectively (Figure 7A). The increase in body weight was likely driven by increased adipose tissue mass, which was significantly higher in the MSDC-0602K-fed group compared to vehicle-treated obese rats (Supplementary Fig. 6A). However, obese rats fed MSDC-0602K had a significant reduction in liver weight and hepatic triglycerides compared to vehicle-fed obese rats (Supplementary Figs. 6B–C). Interestingly, these findings are similar to previous work showing that individuals treated with MSDC-0602K displayed elevated body weight and a significant reduction in hepatic steatosis [3]. Vehicle-fed *fa/fa* rats had a 2.7-fold increase in fasting blood glucose concentrations and 4.2-fold increase in HOMA-IR, whereas both glucose and HOMA-IR in MSDC-0602K-fed obese rats were not significantly different from lean rats (Figure 7B–C). Plasma triglyceride concentrations were also similar between obese MSDC-0602K-fed and lean rats, whereas vehicle-fed obese rats had a 7.2-fold increase in circulating triglycerides relative to lean rats (Figure 7D).

Hepatic pBCKDH abundance was variable in vehicle-treated *fa/fa* rats and only a trend towards increased pBCKDH compared to *fa/+* rat liver was detected. However, pBCKDH content tended to be decreased with MSDC-0602K treatment compared to vehicle treated *fa/fa* rats (Figure 7E–F). We found that hepatic pACLY was increased by 2.8-fold in MSDC-0602K-fed rats, relative to lean controls, but pACC was decreased in MSDC-0602K-fed compared to vehicle-treated obese rats (Figure 7E–F). Previous studies have shown that extrahepatic tissues are also highly involved in BCAA catabolism [41], including brown adipose tissue (BAT), skeletal muscle, and heart. However, we observed no major differences in pBCKDH levels between vehicle-fed and MSDC-0602K-fed rats in these tissues (Supplementary Figs. 6A–C).

Plasma concentrations of valine, isoleucine, and total BCAAs were elevated in both vehicle- and MSDC-0602K-fed obese rats, relative to lean rats, whereas leucine levels were only statistically increased in vehicle-fed rats (Figure 7G). Plasma BCKAs and pyruvate tended to be decreased in *fa/fa* vehicle vs *fa/+* vehicle rats and tended to be increased in MSDC-0602K-fed vs vehicle-fed *fa/fa* rats (Supplementary Figs. 6D–E). Interestingly, the BCKA metabolite 3-hydroxybutyrate (3-HIB), which has been shown to promote insulin resistance in mice [42], was increased by ~2.1-fold in vehicle-fed *fa/*

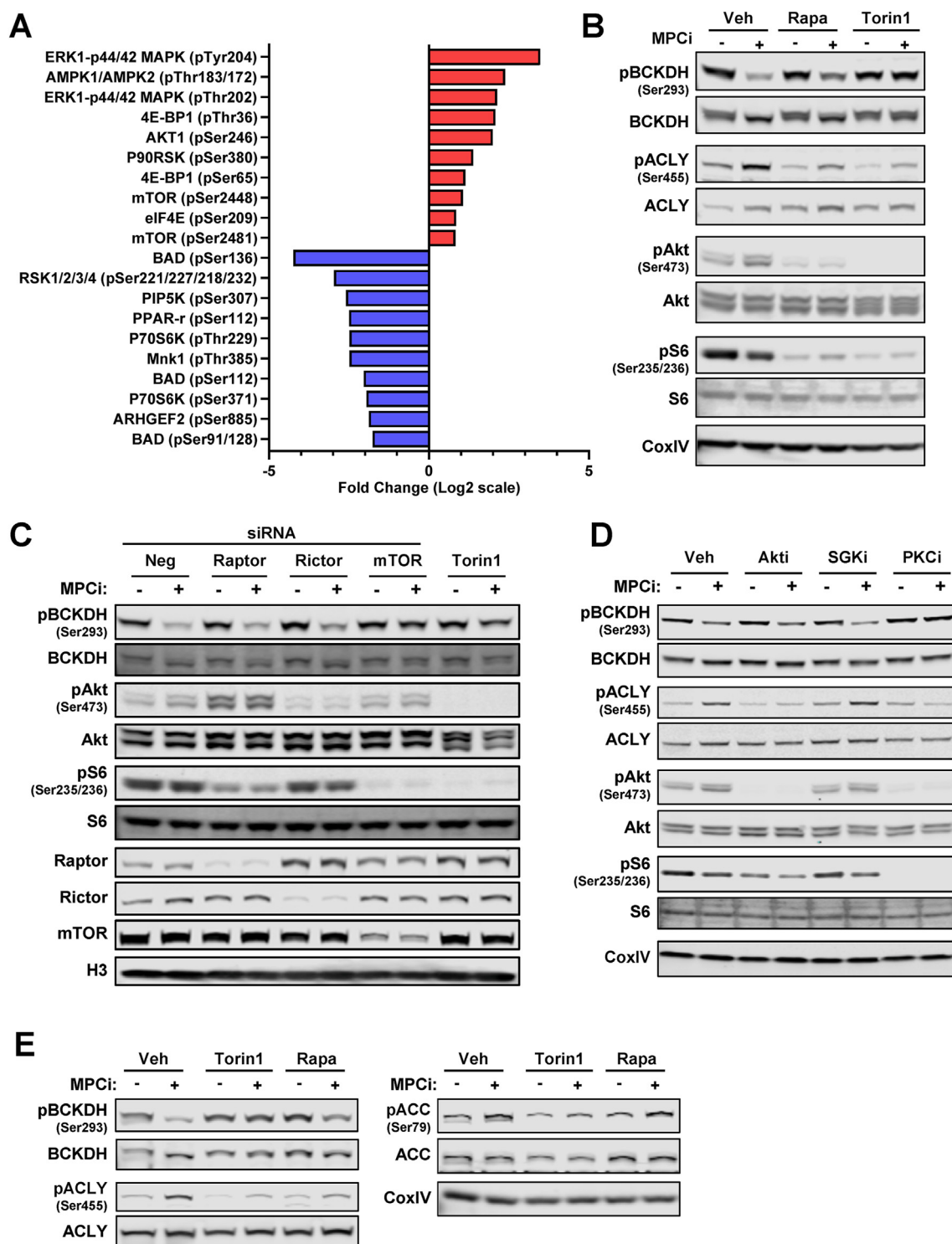


Figure 5: MPCi treatment activates mTORC2 signaling, which is required for reduced pBCKDH. Huh7 cells treated with either Veh (DMSO) or MPCi (UK5099, 2.5 μ M) were harvested and used for analysis of signaling with an mTOR phosphoarray (described in methods). (A) The top 10 positively and negatively regulated phospho-sites measured are represented. Data are expressed as the fold change (Log2 scale) of the MPCi-treated group (phospho-antibody/total antibody) versus the Veh-treated group (phospho-antibody/total antibody). (B) Representative western blots of cells treated with either Veh (DMSO), Rapamycin (10 nM), or Torin1 (250 nM), in the presence of either Veh or MPCi (7ACC2, 2.5 μ M). (C) Cells were transfected with indicated siRNA, then 48 h later were treated with either Veh, MPCi (7ACC2, 2.5 μ M), or Torin1 (250 nM) overnight. (D) Representative western blots of cells treated with either Veh (DMSO), AKT inhibitor (Akti; MK2206, 500 nM), SGK inhibitor (SGKi; SGK1 inhibitor, 500 nM), or PKC inhibitor (PKCi; Rottlerin, 2.5 μ M), in the presence of either Veh or MPCi (UK5099, 2.5 μ M). (E) Representative western blots of cells treated with either Veh (DMSO), Torin1 (250 nM), or Rapamycin (10 nM), in the presence of either Veh or MPCi (7ACC2, 2.5 μ M).

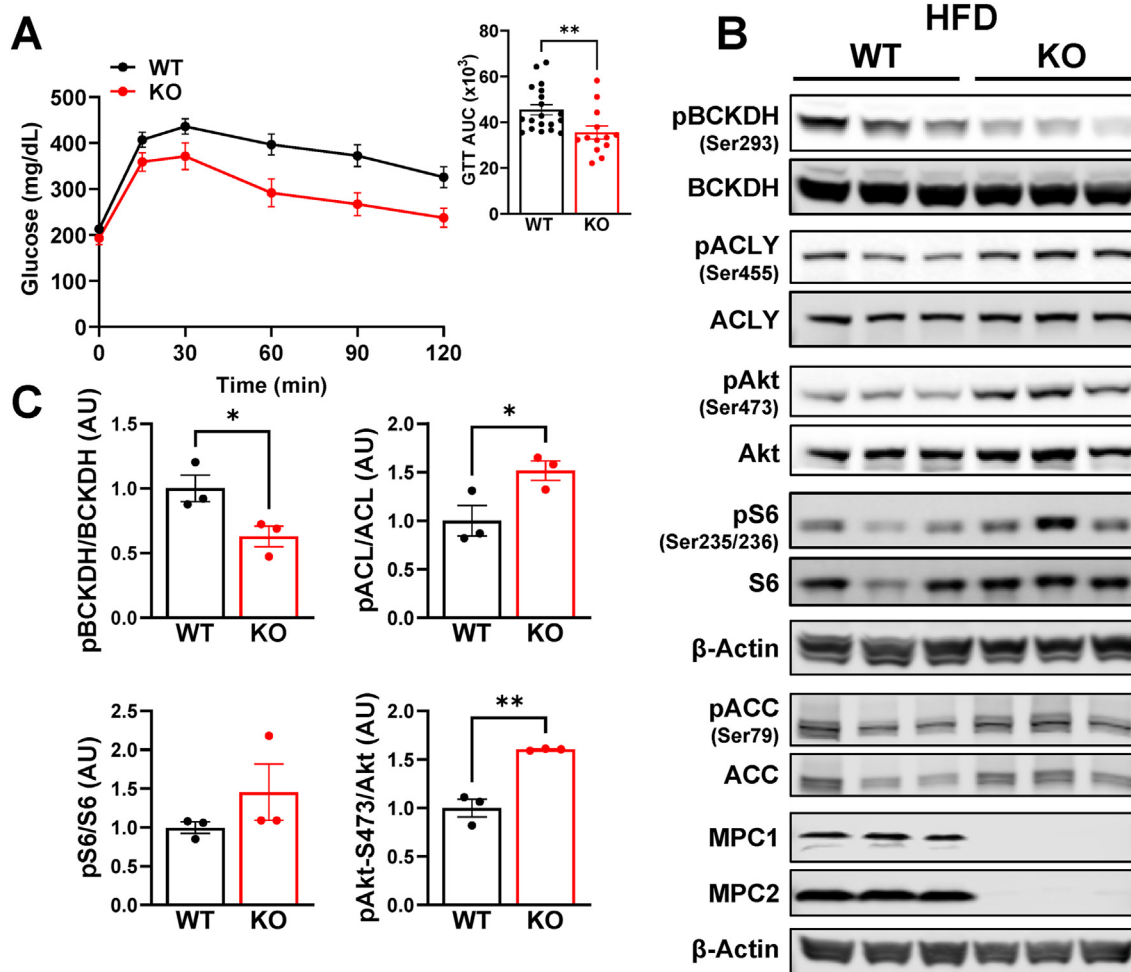


Figure 6: Genetic deletion of the MPC in liver of mice reduces BCKDH phosphorylation. A and B, WT and LS-*Mpc2*^{-/-} mice were fed a 60% high fat diet for 20 weeks. (A) Following a 5-hour fast glucose tolerance was assessed ($n = 13-19$). (B) Representative western blot images of hepatic protein expression. (C) Densitometric analysis of band intensity of pBCKDH-S293/BCKDH, pACLY-S455/ACLY, pS6-S235/236/S6, and pAkt-S473/Akt ratio ($n = 3$). All data are expressed as mean \pm SEM. * $p < 0.05$, ** $p < 0.01$.

fa rats compared to lean controls, but MSDC-0602K feeding corrected this effect (Figure 7H). Lastly, compared to lean rats, the BCAA metabolites C3- and C5-acylcarnitines were reduced in both vehicle- and MSDC-0602K-fed obese rats, but MSDC-0602K feeding significantly increased C3-acylcarnitines relative to vehicle-fed fa/fa rats (Figure 7H). Collectively, these data suggest that improvements in glucose and lipid homeostasis elicited by MSDC-0602K in rats are associated with some alterations in BCAA metabolism, but not a correction in plasma BCAA concentrations.

4. DISCUSSION

In recent years, pharmacologic or genetic inhibition of the MPC in liver has demonstrated promise for treating metabolic diseases such as insulin resistance, type 2 diabetes mellitus (T2DM), and NASH in both animal models and in clinical trials [1–5]. Although plausible mechanisms of action for the effectiveness of MPCi in these diseases have been identified, other possibilities remain to be explored. In the current work, we investigated the possible effects of MPC inhibition on BCAA metabolism, which is dysregulated in insulin resistance and T2DM, and further dissected the mechanisms taking place. Herein we show that patients with NASH, treated with the MPCi MSDC-0602K, had

marked reductions in plasma BCAA levels, which coincided with improvements in plasma glucose, insulin, and adiponectin concentrations. Mechanistically, we found that genetic or pharmacologic inhibition of the MPC leads to reduced phosphorylation of BCKDH that is possibly secondary to diminished intramitochondrial pyruvate and mediated by the PPM1K phosphatase. Collectively, our work indicates a novel mechanism whereby MPCi modulate the cross talk between mitochondrial pyruvate and BCAA metabolism, and enhance BCKDH activity via PPM1K to lower plasma BCAA concentrations.

Multiple metabolomic studies have demonstrated that plasma BCAA, and related metabolites, are highly correlated with insulin resistance, T2DM, and the risk of future development of T2DM in humans [10–14]. However, whether BCAA levels promote insulin resistance, or are simply a consequence of the disease, is still a matter of debate. Indeed, reports correlating elevated BCAA levels to increased serum insulin, in patients with obesity, suggested that elevated levels were likely a secondary manifestation of obesity since amino acid levels decreased upon weight loss [10,43]. On the other hand, genome-wide association studies have linked genetic variations in enzymes that control BCAA metabolism [19,20,44], especially PPM1K [20], to plasma BCAA levels and insulin resistance and dietary restriction of BCAA in ZDF rats lowers plasma BCAAs and improves insulin

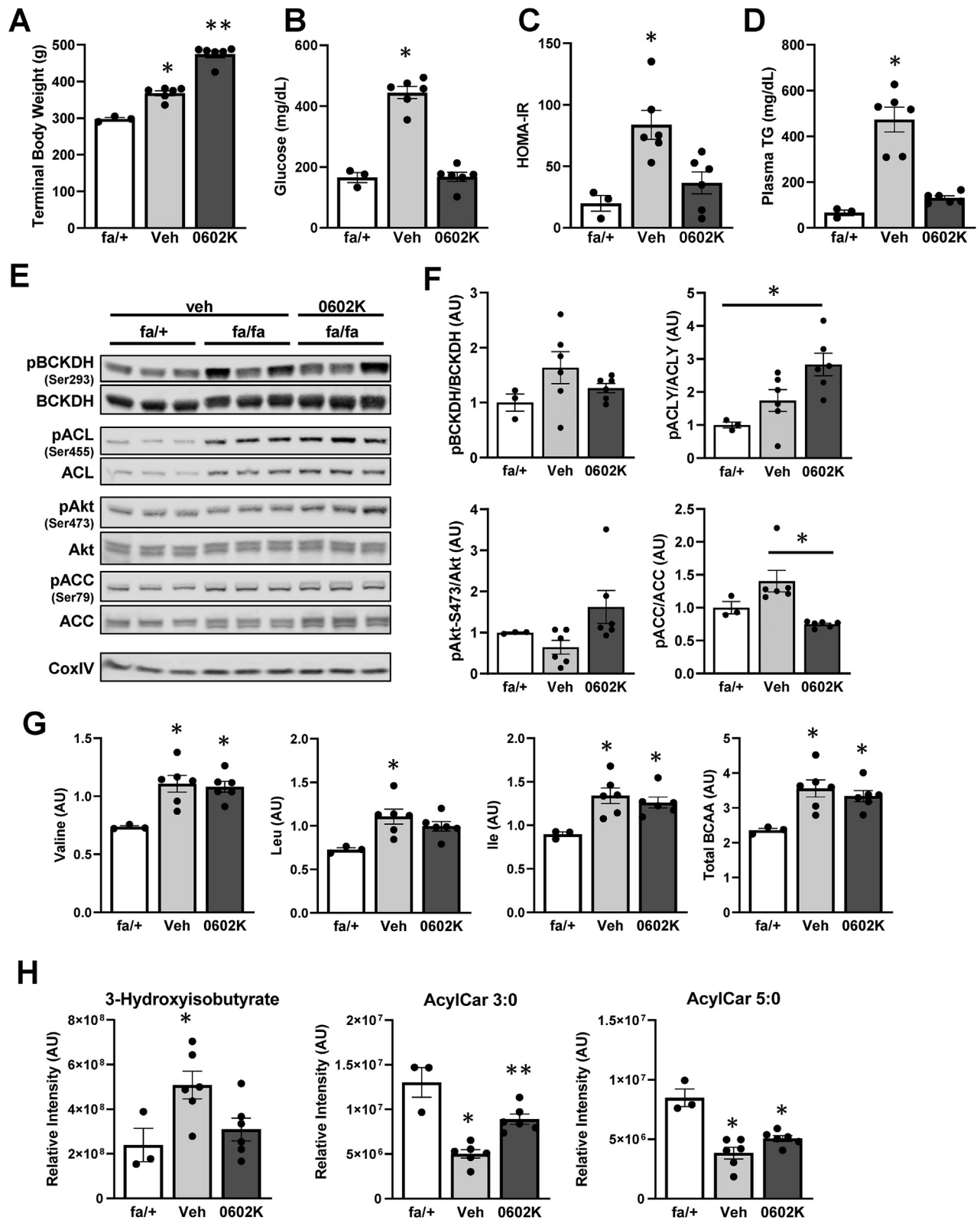


Figure 7: Pharmacological MPC inhibition in diabetic rats improves hyperglycemia. Obese (fa/fa) Zucker diabetic fatty (ZDF) rats were placed on either a standard rodent chow (Veh) or rodent chow containing MSDC-0602K (0602K) for a period of 3 weeks, along with lean (fa/+) controls. (A) Assessment of terminal body weight after 3 weeks of diet. Measurements of (B) glucose, (C) HOMA-IR (calculated from fasting levels of glucose and insulin [51]), and (D) plasma triglycerides (TG) from plasma of rats following a 5 h fast. (E) Representative western blot images of hepatic protein expression. (F) Densitometric analysis of band intensity of pBCKDH-S293/BCKDH, pACL-S455/ACL, pAkt-S473/Akt, and pACC-S79/ACC ratio. (G) Relative abundances of individual and total circulating BCAAs. (H) Relative abundances of circulating 3-hydroxybutyrate, C3-acylcarnitine, and C5-acylcarnitine. All data are expressed as mean \pm SEM (n = 3–6). *p < 0.05 vs control (fa/+), **p < 0.05, Veh vs MSDC-0602K.

sensitivity [18], suggesting that high BCAA concentrations play a causative role in the development of insulin resistance. Herein, we report that treatment with an insulin sensitizing MPCi lowers plasma BCAA in people with NASH in association with marked reductions in plasma glucose and insulin concentrations. However, in rats, improvements in blood glucose and triglyceride concentrations with MPCi treatment were not associated with lower plasma BCAA content, but were associated with reversal of obesity-related changes in the circulating BCAA metabolites 3-HIB and C3 acylcarnitine. While the present studies cannot clarify the cause-and-effect relationship between BCAAs and insulin resistance in people, they are consistent with another study demonstrating that an insulin sensitizing agent and known MPCi, pioglitazone, also lowers plasma BCAAs in people with NASH [45].

Circulating BCAA are increased in Zucker diabetic fatty rats (ZDF), which is believed to be mediated by reduced levels of PPM1K and increased hepatic BDK activity, which leads to increased pBCKDH and impaired BCKA oxidation [18,22,23]. In contrast, diet-induced obese mice were found to have no change in plasma BCAA [46]. This may be explained by species differences in the regulation of BDK, since mice lack a carbohydrate response element binding protein binding site in the BDK promoter that is present in rats and humans [24]. However, there are some reports that mice with leptin or leptin receptor mutations exhibit elevated plasma BCAA concentrations [22,23,28]. In the present study, we found that *db/db* mice exhibit increased hepatic pBCKDH, which was reduced in *db/db* LS-*Mpc2*^{-/-}; however, we did not see a dramatic decrease in circulating BCAAs between *fl/fl* and LS-*Mpc2*^{-/-} on the *db/db* background (Supplemental Fig. 5). It is possible that the effects on BCKDH phosphorylation, seen with hepatocyte-specific *Mpc2* deletion, are not sufficient to enhance BCKA catabolism to a degree that results in reduced circulating BCAAs. The effects of pharmacologic MPCi on BCAAs may be more dramatic because they are not liver-specific and could enhance BCKA oxidation in other organs that have high rates of BCKA catabolism. Indeed, a recent study with BDK liver-specific knockout mice demonstrated that this was not sufficient to affect systemic BCAA concentrations, but that systematic BDK inhibition lowered BCAAs by enhancing oxidation in extrahepatic tissues [47]. In the rat study described herein, we did not find an effect of MPCi on BCKDH phosphorylation in heart, BAT, or skeletal muscle and only a trend towards reduced pBCKDH in liver. It should be noted that the pBCKDH content of *fa/fa* liver was not elevated compared to *fa/+* due to individual rat variability. Concordantly, with the lack of change in multi-tissue pBCKDH content, plasma BCAA concentrations were not affected by MPCi treatment, but changes in BCAA downstream metabolite content were detected. It is possible that the dose and duration of treatment was insufficient to lower BCAA, but the three-week treatment corrected obesity-related derangements in plasma triglyceride and glucose concentrations as well as improving the HOMA-IR. These findings suggest that MPCi-mediated improvements in glucose and HOMA-IR can occur independently of reduced BCAA. We cannot exclude the possibility that alterations in downstream BCAA metabolites, which could be mediators of insulin resistance [42], play a role in the response to MPCi, since 3-HIB and C3 acylcarnitine were corrected by MSDC-0602K.

The present findings describe metabolic crosstalk between mitochondrial pyruvate and BCKA metabolism. Our model suggests that high intramitochondrial pyruvate abundance leads to increased pBCKDH. This is supported by evidence that supplementation of pyruvate increases pBCKDH, but that this can be counteracted by MPCi or enhancing pyruvate oxidation with DCA. These effects on BCKDH covalent modification are consistent with biochemical data generated

many years ago by the Olson group [31,32]. In those studies, they found that addition of pyruvate suppressed ¹⁴C-BCKA oxidation in heart and that DCA and an early MPCi (α -cyanocinnamate) could prevent the effects of exogenous pyruvate on BCKA oxidation [31]. At that time, the regulation of BCKDH activity by phosphorylation had yet to be discovered and was therefore not assessed. The present studies are quite consistent with these historic findings and add additional mechanistic insight including demonstration that the effects of pyruvate and MPCi are likely mediated by the phosphorylation status of BCKDH and require PPM1K activity.

The mitochondrial phosphatase PPM1K is known to bind to the E2 subunit of the BCKDH complex, and dephosphorylate the E1 alpha subunit at serine 293 to increase BCKDH activity [48]. Mutations in the gene encoding PPM1K lead to maple syrup urine disease in people, which is characterized by high urinary excretion of BCAAs and BCKAs due to impaired BCKA oxidation [49]. The gene encoding PPM1K is transcriptionally regulated in HepG2 cells and is downregulated in media without BCAA [50], but we saw no effect of MPCi on the abundance of PPM1K protein. Further investigation will be required to understand the relationship between MPCi and PPM1K.

Analysis of metabolite abundance revealed a trend towards increased BCAA catabolites (hydroxyisobutyrate, propionyl CoA, methylmalonyl CoA) and a substantial decrease in various TCA intermediates in MPCi-treated cells. Reduction in TCA intermediate abundance could be expected since MPCi block an important step in the complete oxidation of glucose by impeding pyruvate entry into the mitochondria. Increased BCKDH activity and BCAA catabolites could be a compensatory mechanism to provide alternative substrates to replenish TCA intermediates. Accordingly, we found MPCi-treated cells had elevated levels of AMP, ADP, and an increase in the ratio of AMP/ATP, which is known to activate AMPK, a critical regulator of energy homeostasis. Indeed, MPCi led to enhanced AMPK activity as evidenced by greater phospho-AMPK α at threonine 172, as well as a downstream target of AMPK, phospho-ACC at serine 79 [33]. The role of AMPK was further demonstrated by the addition of dorsomorphin, an AMPK inhibitor, which blunted the effects of MPCi on pBCKDH in Huh7 cells. This may be an effect that is relevant only to our *in vitro* studies, since we did not observe an increase in phospho-ACC serine 79 *in vivo* with MPC inhibition or deletion. It is possible that the *in vitro* conditions used led to a relative depletion of key energy substrates since glutamine supplementation attenuated the signaling effects of MPCi on AMPK and pBCKDH.

Several observations suggest that selective activation of mTORC2 by MPCi is an important facet of the response to this compound both *in vitro* and *in vivo*. We found increased phosphorylation of the mTORC2 target Akt, at serine 473, and ACLY at serine 455, which is a substrate of Akt [37], in hepatoma cells and in liver of diet-induced obese LS-*Mpc2*^{-/-} mice and ZDF rats. Mechanistic studies revealed that the addition of Torin1, which inhibits both mTORC1 and mTORC2, diminished the effects of MPCi on pBCKDH, while Rapamycin, which somewhat selectively inhibits mTORC1, had a much lesser effect. Knockdown of the mTOR kinase itself, via siRNA, reversed the effect of MPCi on pBCKDH. However, knockdown of the regulatory components of mTORC1 (Raptor) or mTORC2 (Rictor) did not alter MPCi-mediated pBCKDH reduction. These data could suggest that signaling through either mTORC1 or mTORC2 is sufficient to mediate the metabolic crosstalk. Alternatively, a non-canonical mTOR complex (mTORC3), which has previously been suggested to exist [38], could mediate the response. In contrast to AMPK signaling, the effects of MPCi on mTOR activity were observed both *in vitro* and *in vivo*. It is likely that this is the critical component this metabolic crosstalk in response to MPCi. Our studies indicate that MPCi enhances BCKDH

phosphorylation in a manner that is dependent on mTOR, but further work will be needed to identify additional downstream mediators that connect mTOR to altered BCKDH phosphorylation.

5. CONCLUSION

To conclude, we show that use of the MPCi MSDC-0602K, in people with NASH, led to marked improvement in insulin sensitivity and glycemia, which was accompanied by substantial decreases in circulating BCAA levels. Furthermore, phosphorylation of BCKDH, which inactivates the rate-limiting enzyme in BCAA catabolism, was decreased in human hepatoma cell lines treated with MPCi, which was mediated by the phosphatase PPM1K. Activation of pyruvate oxidation mimicked the effect of MPCi, suggesting that MPCi may enhance BCKDH activity by reducing intramitochondrial pyruvate accumulation. Addition of MPCi led to elevated AMP levels and an increase in phosphorylation of downstream targets of AMPK and mTORC2, while inhibition of these kinases abolished the effects of MPCi on pBCKDH in vitro. Phosphorylation of BCKDH was decreased, and downstream mTOR targets (Akt and ACLY) were increased in the liver of obese *LS-Mpc2^{-/-}* mice, and a trend towards similar changes was observed with pharmacological MPCi in obese rats. Collectively, these data reveal cross talk between BCAA metabolism and mitochondrial pyruvate, and provide evidence that inhibition of the MPC leads to reduced circulating BCAA levels and hepatic BCKDH phosphorylation in a manner that is dependent on AMPK/mTOR signaling.

CONFLICT OF INTEREST

BNF is a shareholder and a member of the Scientific Advisory Board for Cirius Therapeutics, which is developing an MPC modulator for treating nonalcoholic steatohepatitis. JRC is the co-founder and part owner of Metabolic Solutions Development and Cirius Therapeutics which are developing clinical candidates including this class of potential therapeutics

DATA AVAILABILITY

Data will be made available on request.

ACKNOWLEDGMENTS

This work was funded by NIH grants R01 DK104735 and R01 DK117657 (to B.N.F.). The Core services of the Diabetes Research Center (P30 DK020579), Digestive Diseases Research Cores Center (P30 DK052574), and the Nutrition Obesity Research Center (P30 DK56341) at the Washington University School of Medicine also supported this work. D. F. was supported by a training grant (T32 DK007120). N.K.H.Y. was supported by a training grant (T32 HL134635). K.S.M. was supported by (R00 HL136658). Some metabolic analyses were supported by NIH grant R35 ES028365 (to G.J.P.). The Washington University Metabolomics Facility conducted mouse plasma metabolomic analyses. The authors would like to thank Margery A. Connelly (LabCorp) for NMR-based analysis of amino acids in people.

APPENDIX A. SUPPLEMENTARY DATA

Supplementary data to this article can be found online at <https://doi.org/10.1016/j.molmet.2023.101694>.

REFERENCES

- [1] McCommis KS, Chen Z, Fu X, McDonald WG, Colca JR, Kletzien RF, et al. Loss of mitochondrial pyruvate carrier 2 in the liver leads to defects in gluconeogenesis and compensation via pyruvate-alanine cycling. *Cell Metabol* 2015;22(4):682–94.
- [2] McCommis KS, Hodges WT, Brunt EM, Nalbantoglu I, McDonald WG, Holley C, et al. Targeting the mitochondrial pyruvate carrier attenuates fibrosis in a mouse model of nonalcoholic steatohepatitis. *Hepatology* 2017;65(5):1543–56.
- [3] Harrison SA, Alkhoury N, Davison BA, Sanyal A, Edwards C, Colca JR, et al. Insulin sensitizer MSDC-0602K in non-alcoholic steatohepatitis: a randomized, double-blind, placebo-controlled phase IIb study. *J Hepatol* 2020;72(4):613–26.
- [4] Gray LR, Sultana MR, Rauckhorst AJ, Oonthonpan L, Tompkins SC, Sharma A, et al. Hepatic mitochondrial pyruvate carrier 1 is required for efficient regulation of gluconeogenesis and whole-body glucose homeostasis. *Cell Metabol* 2015;22(4):669–81.
- [5] Rauckhorst AJ, Gray LR, Sheldon RD, Fu X, Pewa AD, Feddersen CR, et al. The mitochondrial pyruvate carrier mediates high fat diet-induced increases in hepatic TCA cycle capacity. *Mol Metabol* 2017;6(11):1468–79.
- [6] Herzig S, Raemy E, Montessuit S, Veuthey JL, Zamboni N, Westermann B, et al. Identification and functional expression of the mitochondrial pyruvate carrier. *Science* 2012;336(6090):93–6.
- [7] Bricker DK, Taylor EB, Schell JC, Orsak T, Boutron A, Chen YC, et al. A mitochondrial pyruvate carrier required for pyruvate uptake in yeast, *Drosophila*, and humans. *Science* 2012;337(6090):96–100.
- [8] Petersen MC, Shulman GI. Mechanisms of insulin action and insulin resistance. *Physiol Rev* 2018;98(4):2133–223.
- [9] Hodges WT, Jarasvarapam C, Ferguson D, Griffett K, Gill LE, Chen Y, et al. Mitochondrial pyruvate carrier inhibitors improve metabolic parameters in diet-induced obese mice. *J Biol Chem* 2022;298(2):101554.
- [10] Felig P, Marliss E, Cahill Jr GF. Plasma amino acid levels and insulin secretion in obesity. *N Engl J Med* 1969;281(15):811–6.
- [11] Thalacker-Mercer AE, Ingram KH, Guo F, Ilkayeva O, Newgard CB, Garvey WT. BMI, RQ, diabetes, and sex affect the relationships between amino acids and clamp measures of insulin action in humans. *Diabetes* 2014;63(2):791–800.
- [12] Palmer ND, Stevens RD, Antinozzi PA, Anderson A, Bergman RN, Wagenknecht LE, et al. Metabolomic profile associated with insulin resistance and conversion to diabetes in the Insulin Resistance Atherosclerosis Study. *J Clin Endocrinol Metab* 2015;100(3):E463–8.
- [13] Newgard CB, An J, Bain JR, Muehlbauer MJ, Stevens RD, Lien LF, et al. A branched-chain amino acid-related metabolic signature that differentiates obese and lean humans and contributes to insulin resistance. *Cell Metabol* 2009;9(4):311–26.
- [14] Menni C, Fauman E, Erte I, Perry JR, Kastenmüller G, Shin SY, et al. Biomarkers for type 2 diabetes and impaired fasting glucose using a nontargeted metabolomics approach. *Diabetes* 2013;62(12):4270–6.
- [15] Wang TJ, Larson MG, Vasan RS, Cheng S, Rhee EP, McCabe E, et al. Metabolite profiles and the risk of developing diabetes. *Nat Med* 2011;17(4):448–53.
- [16] Laferrère B, Reilly D, Arias S, Swerdlow N, Gorroochurn P, Bawa B, et al. Differential metabolic impact of gastric bypass surgery versus dietary intervention in obese diabetic subjects despite identical weight loss. *Sci Transl Med* 2011;3(80):80re82.
- [17] Shah SH, Crosslin DR, Haynes CS, Nelson S, Turer CB, Stevens RD, et al. Branched-chain amino acid levels are associated with improvement in insulin resistance with weight loss. *Diabetologia* 2012;55(2):321–30.
- [18] White PJ, Lapworth AL, An J, Wang L, McGarrah RW, Stevens RD, et al. Branched-chain amino acid restriction in Zucker-fatty rats improves muscle insulin sensitivity by enhancing efficiency of fatty acid oxidation and acylglycine export. *Mol Metabol* 2016;5(7):538–51.
- [19] Wang Q, Holmes MV, Davey Smith G, Ala-Korpela M. Genetic support for a causal role of insulin resistance on circulating branched-chain amino acids and inflammation. *Diabetes Care* 2017;40(12):1779–86.
- [20] Lotta LA, Scott RA, Sharp SJ, Burgess S, Luan J, Tillin T, et al. Genetic predisposition to an impaired metabolism of the branched-chain amino acids

- and risk of type 2 diabetes: a mendelian randomisation analysis. *PLoS Med* 2016;13(11):e1002179.
- [21] Neinast M, Murashige D, Arany Z. Branched chain amino acids. *Annu Rev Physiol* 2019;81:139–64.
- [22] She P, Van Horn C, Reid T, Hutson SM, Cooney RN, Lynch CJ. Obesity-related elevations in plasma leucine are associated with alterations in enzymes involved in branched-chain amino acid metabolism. *Am J Physiol Endocrinol Metab* 2007;293(6):E1552–63.
- [23] Lian K, Du C, Liu Y, Zhu D, Yan W, Zhang H, et al. Impaired adiponectin signaling contributes to disturbed catabolism of branched-chain amino acids in diabetic mice. *Diabetes* 2015;64(1):49–59.
- [24] White PJ, McGarrah RW, Grimsrud PA, Tso SC, Yang WH, Haldeman JM, et al. The BCKDH kinase and phosphatase integrate BCAA and lipid metabolism via regulation of ATP-citrate lyase. *Cell Metabol* 2018;27(6):1281–93. e1287.
- [25] Wolak-Dinsmore J, Gruppen EG, Shalaurova I, Matyus SP, Grant RP, Gegen R, et al. A novel NMR-based assay to measure circulating concentrations of branched-chain amino acids: elevation in subjects with type 2 diabetes mellitus and association with carotid intima media thickness. *Clin Biochem* 2018;54:92–9.
- [26] Helsley RN, Varadharajan V, Brown AL, Gromovsky AD, Schugar RC, Ramachandiran I, et al. Obesity-linked suppression of membrane-bound O-acyltransferase 7 (MBOAT7) drives non-alcoholic fatty liver disease. *Elife* 2019;8.
- [27] Yoshino M, Yoshino J, Smith GI, Stein RI, Bittel AJ, Bittel DC, et al. Worksite-based intensive lifestyle therapy has profound cardiometabolic benefits in people with obesity and type 2 diabetes. *Cell Metabol* 2022;34(10):1431–41. e1435.
- [28] Martino MR, Gutiérrez-Aguilar M, Yiew NKH, Lutkewitte AJ, Singer JM, McCommis KS, et al. Silencing alanine transaminase 2 in diabetic liver attenuates hyperglycemia by reducing gluconeogenesis from amino acids. *Cell Rep* 2022;39(4):110733.
- [29] Adams KJ, Pratt B, Bose N, Dubois LG, St John-Williams L, Perrott KM, et al. Skyline for small molecules: a unifying software package for quantitative metabolomics. *J Proteome Res* 2020;19(4):1447–58.
- [30] Lutkewitte AJ, McCommis KS, Schweitzer GG, Chambers KT, Graham MJ, Wang L, et al. Hepatic monoacylglycerol acyltransferase 1 is induced by prolonged food deprivation to modulate the hepatic fasting response. *J Lipid Res* 2019;60(3):528–38.
- [31] Waymack PP, DeBuysere MS, Olson MS. Studies on the activation and inactivation of the branched chain alpha-keto acid dehydrogenase in the perfused rat heart. *J Biol Chem* 1980;255(20):9773–81.
- [32] Buxton DB, Olson MS. Regulation of the branched chain alpha-keto acid and pyruvate dehydrogenases in the perfused rat heart. *J Biol Chem* 1982;257(24):15026–9.
- [33] Gowans GJ, Hawley SA, Ross FA, Hardie DG. AMP is a true physiological regulator of AMP-activated protein kinase by both allosteric activation and enhancing net phosphorylation. *Cell Metabol* 2013;18(4):556–66.
- [34] Inoki K, Kim J, Guan KL. AMPK and mTOR in cellular energy homeostasis and drug targets. *Annu Rev Pharmacol Toxicol* 2012;52:381–400.
- [35] Kazyken D, Magnuson B, Bodur C, Acosta-Jaquez HA, Zhang D, Tong X, et al. AMPK directly activates mTORC2 to promote cell survival during acute energetic stress. *Sci Signal* 2019;12(585).
- [36] Martinez Calejman C, Trefely S, Entwisle SW, Luciano A, Jung SM, Hsiao W, et al. mTORC2-AKT signaling to ATP-citrate lyase drives brown adipogenesis and de novo lipogenesis. *Nat Commun* 2020;11(1):575.
- [37] Berwick DC, Hers I, Heesom KJ, Moule SK, Tavare JM. The identification of ATP-citrate lyase as a protein kinase B (Akt) substrate in primary adipocytes. *J Biol Chem* 2002;277(37):33895–900.
- [38] Harwood FC, Klein Geltink RI, O'Hara BP, Cardone M, Janke L, Finkelstein D, et al. ETV7 is an essential component of a rapamycin-insensitive mTOR complex in cancer. *Sci Adv* 2018;4(9):eaar3938.
- [39] Ebner M, Sinkovics B, Szczygieł M, Ribeiro DW, Yudushkin I. Localization of mTORC2 activity inside cells. *J Cell Biol* 2017;216(2):343–53.
- [40] Engelsberg A, Kobelt F, Kuhl D. The N-terminus of the serum- and glucocorticoid-inducible kinase Sgk1 specifies mitochondrial localization and rapid turnover. *Biochem J* 2006;399(1):69–76.
- [41] Neinast M, Jang C, Hui S, Murashige DS, Chu Q, Morscher RJ, et al. Quantitative analysis of the whole-body metabolic fate of branched-chain amino acids. *Cell Metabol* 2019;29(2):417–29. e414.
- [42] Jang C, Oh SF, Wada S, Rowe GC, Liu L, Chan MC, et al. A branched-chain amino acid metabolite drives vascular fatty acid transport and causes insulin resistance. *Nat Med* 2016;22(4):421–6.
- [43] Yoshino M, Kayser BD, Yoshino J, Stein RI, Reeds D, Eagon JC, et al. Effects of diet versus gastric bypass on metabolic function in diabetes. *N Engl J Med* 2020;383(8):721–32.
- [44] Mahendran Y, Jonsson A, Have CT, Allin KH, Witte DR, Jørgensen ME, et al. Genetic evidence of a causal effect of insulin resistance on branched-chain amino acid levels. *Diabetologia* 2017;60(5):873–8.
- [45] Kalavalapalli S, Bril F, Koelmel JP, Abdo K, Guingab J, Andrews P, et al. Pioglitazone improves hepatic mitochondrial function in a mouse model of nonalcoholic steatohepatitis. *Am J Physiol Endocrinol Metab* 2018;315(2):E163–73.
- [46] Lee J, Vijayakumar A, White PJ, Xu Y, Ilkayeva O, Lynch CJ, et al. BCAA supplementation in mice with diet-induced obesity alters the metabolome without impairing glucose homeostasis. *Endocrinology* 2021;162(7).
- [47] Bollinger E, Peloquin M, Libera J, Albuquerque B, Pashos E, Shipstone A, et al. BDK inhibition acts as a catabolic switch to mimic fasting and improve metabolism in mice. *Mol Metabol* 2022;66:101611.
- [48] Lu G, Sun H, She P, Youn JY, Warburton S, Ping P, et al. Protein phosphatase 2Cm is a critical regulator of branched-chain amino acid catabolism in mice and cultured cells. *J Clin Invest* 2009;119(6):1678–87.
- [49] Oyarzabal A, Martínez-Pardo M, Merinero B, Navarrete R, Desviat LR, Ugarte M, et al. A novel regulatory defect in the branched-chain α -keto acid dehydrogenase complex due to a mutation in the PPM1K gene causes a mild variant phenotype of maple syrup urine disease. *Hum Mutat* 2013;34(2):355–62.
- [50] Zhou M, Lu G, Gao C, Wang Y, Sun H. Tissue-specific and nutrient regulation of the branched-chain α -keto acid dehydrogenase phosphatase, protein phosphatase 2Cm (PP2Cm). *J Biol Chem* 2012;287(28):23397–406.
- [51] Cifarelli V, Beeman SC, Smith GI, Yoshino J, Morozov D, Beals JW, et al. Decreased adipose tissue oxygenation associates with insulin resistance in individuals with obesity. *J Clin Invest* 2020;130(12):6688–99.